

Incorporation of as-Prepared Eu³⁺-doped Lanthanum Niobate Nanoparticles in Tellurite Glasses

Gislene Batista^{a*} , Valentina Gacha Mendoza^a, Fabia Castro Cassanjes^a, Camila Pereira^a,

Gabriela Simões Freiria^b, Lucas Alonso Rocha^b, Gael Poirier^a

^aUniversidade Federal de Alfenas, Campus de Poços de Caldas, Poços de Caldas, MG, Brasil.

^bUniversidade de Franca, Av. Dr. Armando Salles Oliveira, 201, Pq. Universitário, Franca, SP, Brasil.

Received: August 22, 2023; Revised: October 26, 2023; Accepted: November 07, 2023.

A direct-doping method was tested to design new composite-glasses by incorporating lanthanum niobate nanocrystals (NC) in tellurite glasses. NC powder were grinding with glass powder before heating-quenching, with the main investigation approached of best parameters for NC suitable homogenization but limited dissolution. Thermal analysis signalizes that prior heat-treatment of NC promotes higher transparency and limits NC dissolution. These materials with visually detectable NC aggregates exhibited glass transition temperatures close to the starting glass. LaNbO₄ phase was hardly detected by X-ray diffraction because of the low weight ratio and partial dissolution but the monoclinic polymorph could be identified for lower time. UV-visible-NIR transmission spectra also related progressive lower transparency with light scattering of NC aggregates. Photoluminescence suggest that lower times allowed to ensure the NC environment with lower crystallinity around Eu³⁺-ions in final composite-glass. These results pave the way for designing new materials containing NC not achievable by conventional nucleation-growth methods.

Keywords: Direct-doping, TeO₂, Luminescence, Composite-glass. LaNbO₄

1. Introduction

Although the classic heat-treatment methodology through nucleation and growth steps is well established for the obtaining of nanocrystals (NC) in glassy phases (i.e., a glass-ceramic), the precise choice of NC composition, control of the size distribution and suitable rare earth RE³⁺ doping of these NC cannot always be ensured. In fact, these NC properties are strongly related with the pristine glass composition, thermal history and specific nucleation and growth temperatures and durations in a way that a desired crystalline phase with specific NC size distribution is limited by the own glass composition as well as thermodynamic and kinetic properties of the crystallization process¹⁻⁵. Based on these considerations, an alternative way besides the classical heat-treatment of the pristine glass for the manufacture of glass containing rare-earth doped NC of a desired composition is based on the incorporation of previously prepared NC with suitable properties in the glass matrix. Despite such methodology is a great challenge, several chemical and physical methodologies for NC synthesis are available and are given access to a complete control of the NC composition and average size⁶⁻¹⁰. In this sense, a homogeneous distribution of these NC in complementary glass phase should open opportunities for the design of completely new composite materials, paving the way for innovative applications in electronics and photonics.

Previous works using this incorporation methodology were reported by Zhao et al.² and Zhao and Ebendorff-Heidepriem⁶, which described a method called “direct-doping” to

incorporate light-emitting upconversion nanocrystals (UPNC) (LiYF₄:Yb:Er) in a tellurite glass of composition 75TeO₂-15ZnO-10Na₂O. The method used by the authors consisted by adding the nanocrystals directly in the liquid glass. The authors claim that the classic method by heat treatment, although promising for some types of nanocrystals, presents significant chemical and physical limitations when it comes to RE³⁺-doped nanocrystals, especially for processes involving upconversion. These drawbacks limit the ability to control the system's optical properties and can even lead to increased light dispersion and optical loss in the resulting material^{2,11}. Based on Zhao et al.² and Zhao and Ebendorff-Heidepriem⁶ researches, Nguyen et al.¹¹ applied the direct-doping method using NaYF₄:Yb³⁺:Er³⁺ nanoparticles in glasses of composition 45P₂O₅-(55-x)Na₂O-xNaF (x=0 or 10). Other phosphate glasses compositions were also used as matrix for direct-doping using a series of different Er₂O₃-doped TiO₂, ZnO, and ZrO₂ microparticles. For glasses with the composition 50P₂O₅-40SrO-10Na₂O, a large amount of the particles is thought to dissolve during the glass melting; however, particles were found to survive in glasses with a composition 90NaPO₃-(10-x)Na₂O-xNaF (with x=0 and 10 mol%) due to their lower processing temperature¹². Direct-doping were also used to prepare an oxyfluorophosphate glass-based composites which exhibit green persistent luminescence (PeL) after being UV charged; in which the method should be modified to limit not only the decomposition of the PeL particles in the glass but also the fluorine evaporation occurring during the glass preparation¹³.

*e-mail: gislene.batista@sou.unifal-mg.edu.br

It provides that a key factor for the success of this method is the choice of a suitable incorporation temperature at which nanoparticles do not dissolve at the same time as the glass has adequate viscosity for the dispersion of them, since this methodology added NC powders in the liquid glass composition. Other mandatory parameters are the glass thermal stability against crystallization in order to avoid the nucleating effect of NC on the glass matrix and the high thermal stability (refractory behavior) of the NC composition. In this sense, this type of material obtained by NC incorporation would present several advantages, in particular regarding NC control, such as concentration, composition, size and desired properties. However, the main challenges of the method are related with the establishment of appropriate conditions to ensure the presence of nanocrystals in glass matrix (without or with low dissolution), as well with a high dispersion and homogeneity^{2,6,11,14}.

Thus, this article considers the incorporation of nanocrystals in a glass following these previous works, but with the approach of previous mix the nanocrystals with the glass as a powder instead of adding them in the liquid glass. It's described the preparation and characterization of composite-glasses obtained by the incorporation of crystalline Eu^{3+} -doped lanthanum niobate nanoparticles ($\text{LaNbO}_4:\text{Eu}^{3+}$)¹⁵⁻¹⁸ in tellurite glasses of TeO_2 - GeO_2 - Nb_2O_5 - K_2O - Li_2O system. This system was selected because, among other characteristics, it has low softening temperature and high thermal stability against crystallization. On the other hand, the use of $\text{LaNbO}_4:\text{Eu}^{3+}$ is justified by its high melting temperature (1650°C)¹⁹ and its efficient luminescent properties. Composite-glasses obtained by NC incorporation were investigated by DSC, XRD, UV-Vis-NIR-MIR absorption and photoluminescence.

2. Materials and Methods

2.1. Composite-glass preparation

For composite-glasses preparation, the NC powders and glassy phase were firstly synthesized separately. Tellurite glasses were prepared with molar compositions: 70TeO_2 - 10GeO_2 - $10\text{Nb}_2\text{O}_5$ - $5\text{K}_2\text{O}$ - $5\text{Li}_2\text{O}$ (G1) and 60TeO_2 - 5GeO_2 - $5\text{Nb}_2\text{O}_5$ - $15\text{K}_2\text{O}$ - $15\text{Li}_2\text{O}$ (G2). Glasses were prepared by the conventional melt-quenching method: the powder precursors were weighted in appropriate proportions, grinded in an agate mortar, and subsequently placed in a gold crucible covered with a gold lid and then melted in a furnace. Glass composition G1 was melted at 830°C and glass composition G2 at 800°C, both during 30 minutes. After that step, the melt was quenched into a preheated stainless-steel mold, and then the samples were annealed (300°C - G1 and 210°C - G2) for 10 hours in order to relieve the mechanical stress before slow cooling to room temperature. For optical measurements, some samples were polished using various grades of abrasive paper with ethanol as a solvent and then diamond paste.

The nanocrystals (NC) used for incorporation are lanthanum niobates previously doped with trivalent europium ion - ($\text{La}_{99.75}\text{Eu}_{0.25}$) NbO_4 ^{15,16}. These NC were obtained by spray-pyrolysis process which precursor salts were prepared from their oxides dissolved in hydrochloric acid (HCl 38-36.5%) (LaCl_3 and EuCl_3 , except NbCl_5 salt).

Europium and lanthanum chlorides were added to aqueous solution containing niobium chloride and water (pH: 2.0 - HCl). After homogenized, the solution was placed in the aerosol pyrolysis system in three stages, the first corresponding to the generation of the aerosol from the nebulization using a piezoelectric insert; in the second stage the aerosol generated (drag gas + solvent vapor and the decomposition of products + solid particles) was carried by airflow the heat treatment regions (drying: 100°C and decomposition: 900°C); and in the third stage, the recovery of the powder using an electrostatic filtration. The process time in obtaining the final material is very fast, lasting between 4 to 7 seconds, i.e., the heat treatment time is very short. For this type of synthesis, the final ceramic powder consisted of nanocrystals with diameter around 50 nm aggregated superficially in polydisperse spherical particles^{15,16}.

For composite-glasses preparation, the NC powders and corresponding tellurite glass powders were weighed according to the predetermined mass ratio between nanocrystals and tellurite glass (1% w/w for G1 and 0.5% w/w for G2). Then, the NC powder was gradually incorporated into powdered glass and homogenized in an agate mortar. For this step, the mix of powder glass and NC powder were grinding together for 30 minutes in the mortar. The mixture was transferred to a gold crucible and heated for different times and temperatures. After this step, the material was quenched into a preheated stainless-steel mold and the sample annealed (300 °C/ 10 hours for G1-based material and 210 °C/ 10 hours for G2-based material) before slow cooling to room temperature. For optical measurements of composite-glasses, samples were also polished using various grades of abrasive paper with ethanol as a solvent and then diamond paste. Table 1 presents the synthesis parameters of each sample as well as their nomenclature as follows: precursor glass - incorporation temperature – time in minutes. In addition, the TT index in some of them, corresponds to a heat treatment at 950°C for 10 minutes previously performed on NC before incorporation in the glassy phase.

For composite-glasses prepared with G1 glass composition, 1% w/w of NC was added to the glass powder and the mixture kept at the temperature of 775°C. In fact, this temperature corresponded to the lowest tested temperature at which the glassy phase with a suitable viscosity for pouring in the preheated metallic mold after 5 minutes. This was the main reason for subsequent tests with the G2 glass composition, that containing a higher alkaline content and this way, with an expected lower temperature suitable. In this latter case, the lower temperature/time achieved for a suitable pouring in the mold was obtained for 630°C for 7 minutes. For this set of G2 composite-glasses, samples were also prepared using 700°C for 7 minutes to study the temperature effect on NC survival in the glass. Finally, some of these G2 composite-glasses were also prepared using previously heat-treated NC, such HT step being performed to estimate such parameter on the aggregation/dissolution tendency of NC in the final materials.

2.2. Characterizations

Thermal analysis was performed using a Differential Scanning Calorimeter (DSC) DSC 200F3 Jupiter from




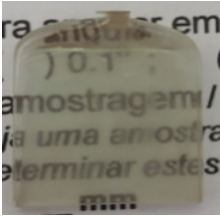

Netzsch on bulk samples of approximately 30 mg in the temperature range of 100 to 590°C, using sealed aluminum pans under a flow of nitrogen atmosphere at 50 cm³.minutes⁻¹ with a heating rate of 10°C.min⁻¹. X-ray diffraction (XRD) data of the powder samples were obtained using a Rigaku Ultima IV diffractometer with CuK α radiation wavelength ($\lambda = 1.5418$ nm), 40kV/30mA, 0.01° step pass, from 10° to 70°. Optical transmission window was measured using an Agilent Technologies Cary 7000 spectrophotometer, from 200 to 2000 nm, and Agilent Cary 630 FTIR in the wavelength region of 2500 - 15000 nm. Refractive indices were acquired indirectly with an ellipsometer Semilab GES 5DS, from the average of three measurements in each sample at different points. Photoluminescence data were obtained at room temperature, under continuous Xe lamp (450W) excitation in a Horiba Jobin Yvon Fluorolog-3 spectrofluorimeter equipped with an excitation and emission

double monochromator and a photomultiplier R 928 Hamatsu at 90° from the incident beam. Emission spectra was obtained with a 394 nm wavelength excitation and Excitation spectra was obtained with a 612 nm wavelength emission. The slits were placed at 2.0 and 1.0 nm for excitation and emission, respectively; the bandpass was 0.3nm, and the integration time was 0.1s. G1227 emission filters were employed. The decay curves were acquired using a phosphorimeter accessory equipped with a pulsed Xe lamp (5J/Pulse).

3. Results and Discussions

Precursor glasses and final composite-glasses (CG) are presented in Table 1. For the G1 sample set, one can notice a clear change in the CG transparency from translucent to transparent samples for longer times at 775°C. On the other hand, in the G2 sample set, all samples are transparent but some NC aggregates can be noticed.

Table 1. Synthesis conditions and visual aspects of pure tellurite glasses and NC-containing composite-glasses.

Glass	Samples	NC composition	Temperature (°C)	Time (min)
G1	 G1-775-05	1% w/w	775	05
	 G1-775-45			45
G2	 G2 _{TT} -630-07	0.5% _{TT} w/w	630	
	 G2-630-07	0.5% w/w		
	 G2 _{TT} -700-07	0.5% _{TT} w/w	700	

Considering that larger particle/aggregate size decreases transparency and increases opacity^{20,21}, it is inferred that longer times promote a higher dissolution of the NC in the glassy phase with related weaker light scattering effects and higher transparency. In a first approximation, NC melting is not expected at such conditions (630-775°C-5min) owing to the high LaNbO_4 melting point of 1650°C¹⁹. However, the dissolution process might be occurring with the NC in the liquid tellurite glass, which is higher as the time increases. Aggregates are observed in G2 composite-glass when NC were previously submitted to heat-treatment (TT index). Such HT, performed at 950°C for 10 minutes, a time longer than the one used in spray-pyrolysis (4-7 seconds)^{15,16}, promotes NC surface aggregation, giving rise to bigger clusters with lower superficial area and resulting in a slower dissolution. Such preliminary results, even though not optimized for transparent CG containing niobate NC, clearly point out that suitable experimental conditions (NC granulometry, NC incorporation ratio, time and temperature, preliminary NC heat-treatment, etc....) can be found for the design of such technological material. Thermal analysis was used in these materials as a tool to monitor glass composition variations. In fact, addition of niobium in tellurite glasses provides a significant increase of glass transition temperature T_g ²²⁻²⁴. Besides, the incorporation into tellurite glass of rare-earth (RE) such as lanthanum and europium increase the presence of non-bridging oxygen (NBO), breaking the Te-O-Te bonding, with the RE replacing the Te and increasing the glass transition temperature²⁵. DSC curves of G1 and G2-based composite-glass bulks are presented in Figure 1 with the value of their respective T_g temperatures. In the G1 series, it clearly appears that increasing times from 5 minutes to 45 minutes promote a T_g increase from 351°C ($T_g=352^\circ\text{C}$ for pure G1 glass) to 362°C. This result is in agreement with a progressive NC dissolution with incorporation of niobium, lanthanum and europium in the tellurite glassy phase. On the other hand, the close values of T_g for the G1 glass and CG prepared with a 5 minutes incorporation time also give an indication that NC have (at least partially) lasted. Such assumption is corroborated by another DSC measurement, for which a powder mixture 2% w/w of NC and pure glassy phase without the process of incorporation was investigated and a T_g value of 348°C was found (versus 347°C for the pure G1 powder). Results obtained for G2 samples is quite similar but the NC dissolution tendency appears to be even more pronounced. In fact, while the pure G2 bulk glass exhibits a T_g temperature at 249°C, the CG sample obtained after 7 minutes at 630°C shows a T_g of 261°C, which suggests again at least a partial incorporation of lanthanum and niobium in the tellurite glass network with resulting higher overall connectivity and higher T_g . Whereas NC dissolution was not detected by DSC in G1 composition for low time (5 min), G2 composition seems to promote a higher dissolution rate for NC, even at lower temperature (630°C). Such behavior can be understood by the higher alkaline content of composition G2 with a resulting lower viscosity at the chosen temperature and higher melting ability. However, an interesting feature is related with the fact that previous heat-treatment of the NC powder apparently hinders dissolution. In fact, this latter CG ($G2_{TT-630-07}$) exhibits a

T_g value of 249°C which is exactly the same value of the pure G2 bulk, while the same composite-glass preparation without prior NC heat-treatment ($G2_{-630-07}$) has a T_g around 261°C. Such HT effect on the NC resistance to dissolution is even efficient at higher temperature since the CG prepared under the same conditions but at 700°C still presents a very close T_g value of 250°C. It is suggested that prior HT could promote structural changes at the NC surface with resulting higher dissolution resistance or promotes NC aggregation with a lower overall surface area as visually observed in these materials (Table 1).

All samples were also characterized by X-ray diffraction as presented in Figure 2. As expected, pure glass samples G1 and G2 do not present any diffraction peak but only the diffraction halo characteristic of non-crystalline materials.

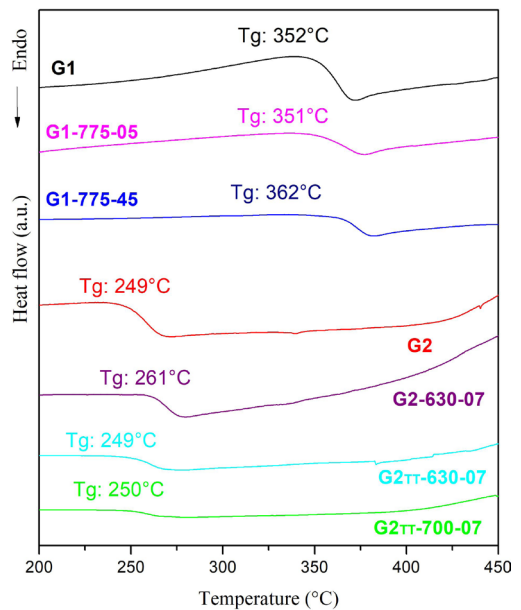


Figure 1. DSC curves of pure tellurite glasses and NC-containing composite-glasses.

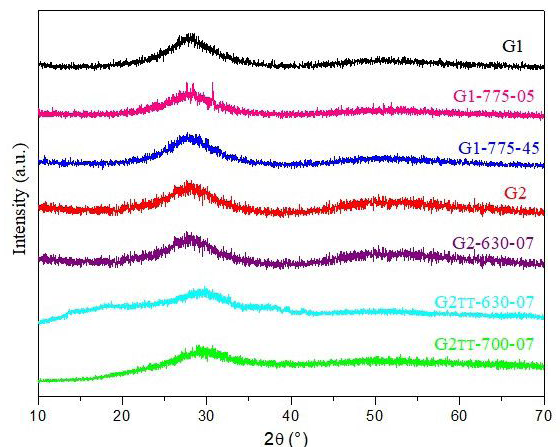


Figure 2. X-ray diffraction patterns of pure tellurite glasses and NC-containing composite-glasses.

Concerning the composite-glass samples, only sample G1-775-05 exhibit clear diffraction peaks as better visualized in Figure 3 between 15 and 40° for this sample and the X-ray diffraction pattern of LaNbO_4 NC powder. It appears that the diffraction peaks identified in the CG are in better agreement with the monoclinic LaNbO_4 phase (PDF: 22-1125) than the tetragonal one (PDF: 50-919) of the starting lanthanum niobate NC^{15,16}. Since LaNbO_4 is a polymorphic material with phase transition between the tetragonal and monoclinic phases in the range $400\text{--}525^\circ\text{C}$ ²⁶⁻²⁸, it is supposed that the high temperature in the liquid glass favors this phase transition. For the other samples that the temperature is higher (G1) or the NC weight ratio is lower (G2), diffraction peaks are no longer identified under these experimental conditions (0.01°/s). In the G1 case, the disappearance of diffraction peaks for longer times is in agreement with an amorphization of the LaNbO_4 NC and at least in part with the dissolution of these NC in the liquid tellurite glass with incorporation of lanthanum and niobium in the tellurite network and resulting higher Tg temperatures. For G2 composite-glass, it is suggested that the lower NC weight ratio of 0.5% stands below the detection limit of the XRD apparatus. But, in fact, it has been shown that prior NC heat treatment seems to hinder the NC dissolution and crystalline aggregates are also easily observed by naked eyes in the material. Since the lack of crystalline peaks for NC-containing glass-ceramics reveals that the such NC do not induce formation of other crystalline phases in the glass under these experimental conditions². Furthermore, unlike conventional glass-ceramics easily characterized by XRD because of a large crystalline volume ratio (typically 25%–35%), NC-doped glasses are hardly identified because of much lower crystalline proportions below the XRD detection limits (around 1 wt%).

Optical windows for the glass and composite-glass samples with their relative transparency in the UV-Vis-NIR-MIR were also determined between 350 and 7000 nm as resumed in Figure 4. First, the cut-off transparency limit of G1 glass is around 410 nm whereas G2 glass has a lower cut-off wavelength (λ) (~360 nm), in agreement with a higher ionic character of this latter composition and substitution of heavy elements by lighter ones^{21,29}. For G1 composite-glass with 1 wt% of NC, short time of 5 minutes clearly decreases the transparency in the visible and near infrared range as previously expected by the translucent aspect of the sample (Table 1), once again suggesting the presence of NC dispersed in the whole sample with associated stronger scattering effects of the incident light. Higher transparency after longer time (45 min) with previously reported higher Tg values are in agreement with dissolution of NC in the tellurite glass matrix. In the G2 series for which the NC w/w ratio is lower, overall transparency in the UV-visible for the G2 pure glass and sample G2_{TT}-630-07 are close as also seen from Table 1, the small difference being attributed to aggregate scattering still identified by naked eyes (Table 1). For the other samples obtained at 700°C (G2_{TT}-700-07), once again in agreement with visual observations from Table 1, was not expected when compared to G2_{TT}-630-07 since the NC w/w ratio is the same. Previous DSC data suggested that NC do not dissolve in a significant extent for both samples. Based on these considerations, one could suggest that higher

temperature promote a higher NC mobility and higher NC agglomeration tendency. From this point of view, bigger particles are expected to promote stronger scattering effects. For all samples, the optical window in the middle infrared is limited to around 6 μm , with two intense absorption bands around 3.3 μm and 4.4 μm attributed to hydroxyl groups OH and CO_2 respectively²¹. Since these absorption bands appeared stronger for the G2 glass and composite-glass, it is suggested that higher alkali contents introduced as carbonate precursors induce a lower chemical stability with more OH terminal bonds as well as CO_2 residual molecules in the final samples.

Figure 5 presents normalized excitation spectra (normalized at the ${}^5\text{L}_6 \leftarrow {}^7\text{F}_0$ transition ~394 nm) for emission at 612 nm for all NC-containing CG, as well as the excitation spectrum of precursor NC powder. Excitation bands depicted in Figure 5 are characteristic of Eu^{3+} and referred to the transitions of states ${}^7\text{F}_{0,1}$ to the excited states ${}^5\text{D}_1$ around 535nm, ${}^5\text{D}_2$ in 464nm, ${}^5\text{D}_3$ in 416nm, ${}^5\text{L}_6$ in 394nm and ${}^5\text{G}_2$ in 382nm^{25,30,31}.

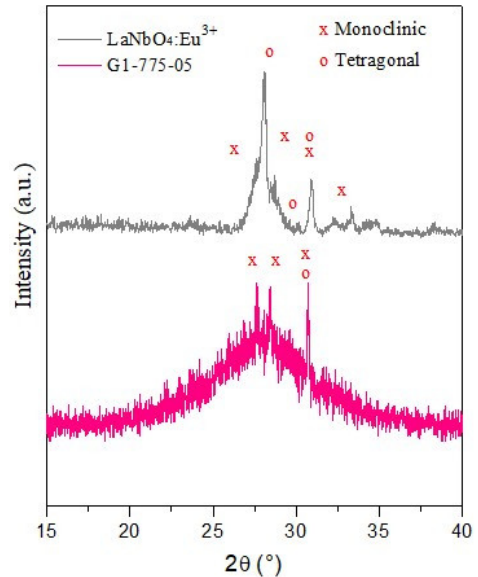


Figure 3. X-ray diffraction patterns of sample G1-775-05 and $\text{LaNbO}_4:\text{Eu}^{3+}$.

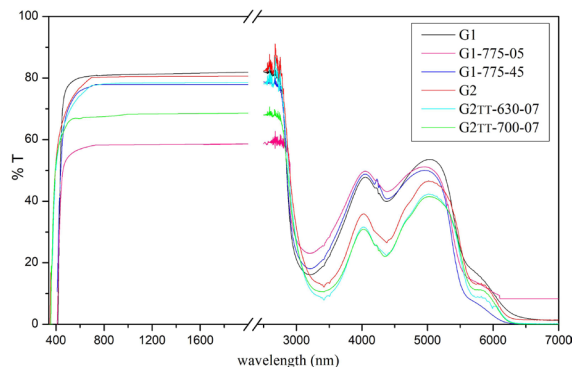


Figure 4. Optical transmission window of pure tellurite glasses and NC-containing composite-glasses.

In the NC emission spectrum, the highest intensity is centered at 394 nm whereas CG from the G1 series exhibit an opposite trend with much higher excitation intensities at 464 nm. As previously established from the UV-Vis-NIR transparency window in Figure 4, the UV-Vis cut-off of these samples is observed around 410 nm in a way that UV excitation at 394 nm is strongly absorbed by the materials and the resulting emission at 612 nm is mainly due to Eu^{3+} ions near the surface. On the other hand, excitation at 464 nm promotes emission of Eu^{3+} from the whole volume. Still, CG from the G2 series exhibit similar emission intensities at 612 nm by both excitations at 394 nm and 464 nm. Following the same reasoning, Figure 4 gives a UV cut-off around 360 nm for these glasses and it must be taken into account that the excitation wavelength at 394 nm is not absorbed in a large extent and promotes excitation of a higher number of Eu^{3+} . However, besides these first considerations, other spectroscopic features must be analyzed in details. In fact, a careful comparison of excitation bands between 375 nm and 425 nm related with transitions from the fundamental state 7F_0 to excited states 5G_2 , 5L_6 and 5D_3 respectively gives a first insight of the Eu^{3+} environment in these samples. Whereas excitation bands from G1 samples exhibit a clear broadening characteristic of amorphous sites, these same excitation bands are better resolved and sharpened for both G2 samples and the NC powder. Such similarity is a clear indication of a more ordered rare-earth environment close to the crystalline lanthanum niobate sites in these G2 composite-glasses. The same spectroscopic trend is also observed for the excitation bands around 530 nm.

Figure 6 presents the emission spectra of the samples under excitation at 394 nm with the characteristic peaks of Eu^{3+} emission, corresponding to transitions from the excited state 5D_0 to the fundamental 7F_J ($J=0,1,2,3$ and 4) with the strongest emission from the ${}^5D_0 \rightarrow {}^7F_2$ transition at 612 nm³⁰⁻³³. Emission bands of the CG exhibit a broadening, probably due to the insertion of Eu^{3+} in distinct atomic sites. Since each Eu^{3+} environment produces an emission at a specific wavelength, several emission sites result in several elemental emission bands observed as a broadened overall band²¹. In agreement with previous thermal and optical data, it appears from these emission spectra that at least part of Eu^{3+} ions are inserted in a highly distorted environment such as a vitreous structure, in agreement with a partial dissolution of the NC. However, emission bands collected from samples G2_{TT}-630-07 and G2_{TT}-700-07, although broader than for pure LaNbO_4 NC, are slightly narrower when compared to the samples from the G1 series.

Besides optical applications as a red emitter, Eu^{3+} is also widely used as a structural probe because of very specific electronic transition properties of this ion³⁰⁻³³. Figure 7 presents these emission spectra normalized at the ${}^5D_0 \rightarrow {}^7F_1$ transition (~ 590 nm) for a better comparison with the relative intensity of the ${}^5D_0 \rightarrow {}^7F_2$ transition at 612 nm. In fact, the ${}^5D_0 \rightarrow {}^7F_1$ is a magnetic dipole (MD) transition and the environment surrounding Eu^{3+} almost not affects its intensity. On the other hand, the ${}^5D_0 \rightarrow {}^7F_2$ is an electric dipole (ED) transition that is hypersensitive to the environment around the ions. Therefore, the intensity ratio of these two transitions (or asymmetry ratio) gives an indication of the

symmetry around Eu^{3+} ³⁰⁻³³. From a first overall analysis of Figure 7, the asymmetry ratio is high for all CG samples and even for pure NC, suggesting that Eu^{3+} is surrounded by a low symmetry environment even in crystalline LaNbO_4 . In addition, the appearance of the ${}^5D_0 \rightarrow {}^7F_0$ transition, even with a weak intensity, points out again the presence of a low symmetry environment^{15,16,30-33}. A more detailed analysis of emission spectra in Figure 7 also brings important structural information between G1 e G2 samples sets. First, the asymmetry ratio decreases from G1 to G2 samples as detected by a progressive lower intensity of the ${}^5D_0 \rightarrow {}^7F_2$ transition.

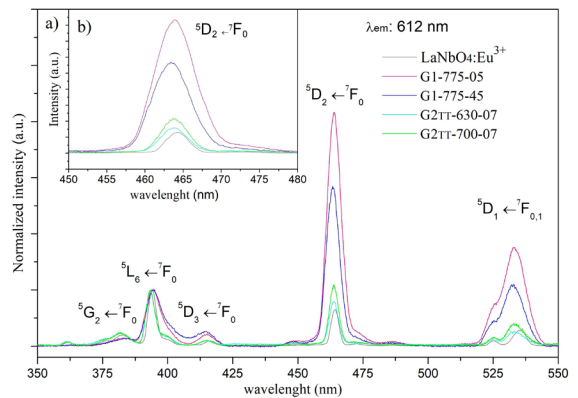


Figure 5. Excitation spectra normalized in ${}^5L_6 \leftarrow {}^7F_0$ transition (~ 394 nm) of NC-containing composite-glasses and $\text{LaNbO}_4:\text{Eu}^{3+}$ ($\lambda_{\text{em}} = 612$ nm) (a) and ${}^5D_2 \leftarrow {}^7F_0$ transition of the same spectra (b).

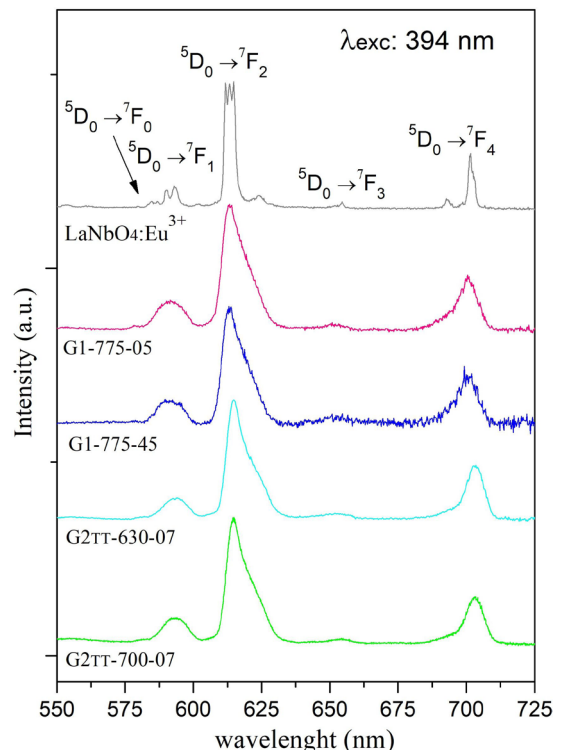


Figure 6. Emission spectra of NC-containing composite-glasses, and $\text{LaNbO}_4:\text{Eu}^{3+}$ ($\lambda_{\text{exc}} = 394$ nm).

Besides, as already pointed, the emission bands from the $^5D_0 \rightarrow ^7F_1$ transition centered at 590 nm are narrower for G2 samples. Both spectral information are in agreement with a less distorted environment around Eu³⁺ ions in G2 samples and support the previous hypothesis that crystalline lanthanum niobate NC were not completely dissolved in these samples. Thus, one can suggest that the outer part of NC contained in G2 samples have dissolved, whereas the inner part remains crystalline under these experimental synthesis conditions. In such a situation, part of Eu³⁺ ions are still incorporated in the crystalline LaNbO₄ structure whereas Eu³⁺ ions from the outer part of NC were dissolved in the surrounding tellurite glass network or experiment an amorphous lanthanum niobate environment.

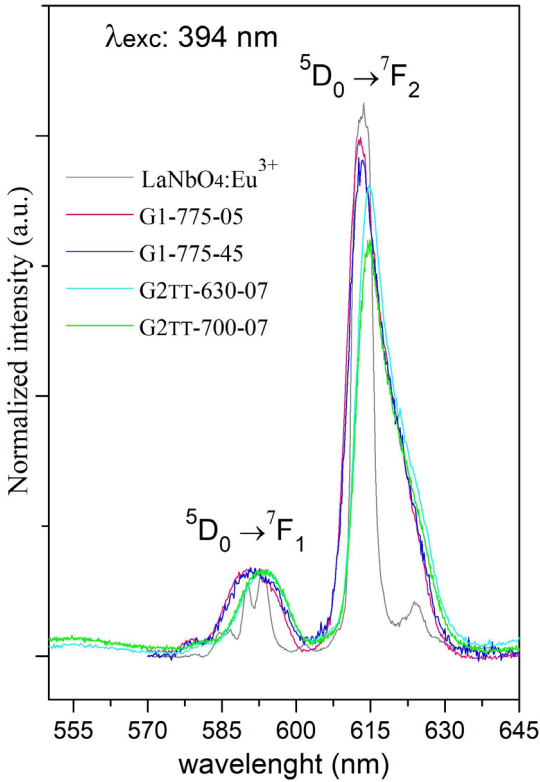


Figure 7. Emission spectra of NC-containing composite-glasses and LaNbO₄:Eu³⁺, normalized in $^5D_0 \rightarrow ^7F_1$ (~590nm) transition ($\lambda_{exc} = 394$ nm).

Experimental lifetime values (τ) presented in Table 2 (as well as refractive indices) were found by a first order exponential adjustment ($I = I_0 e^{(-1/\tau_{exp})t}$ in which I represent the intensity at time t, I_0 represent the intensity at time t_0 and τ_{exp} is the lifetime for the 1/e decay of the population after the end of the excitation) from decay curves under excitation at 394 nm and emission at 612 nm. The use of the monoexponential adjustment is justified by corresponding to an average of all sites with similar optical properties, since distinct Eu³⁺ sites can only be identified using lifetimes if the radiative decay in both sites is different i.e., optical properties around the luminescent ion (refractive index and phonon energy). Otherwise, a monoexponential adjustment will accurately fit the radiative decay data. As an example, LaNbO₄ NC are known to possess more than one Eu³⁺ symmetry center due to the mixture of phases^{16,34}. According to Freiria's analysis¹⁶, heat-treated NC powders presented a lifetime of 0.78 ± 0.08 ms under the same experimental conditions. In the case of our materials, some data obtained by monoexponential fit exhibited a low-quality factor R² (Table 2). However, further adjustments using higher order exponentials did not give better quality factors because of a high dispersion of values, such behavior being attributed to the multiple Eu³⁺ sites ranging from a crystalline LaNbO₄ environment to an alkali tellurite glassy network.

For the G1 set of samples reported in Table 2, experimental lifetimes fit around 0.72 ms within the error analysis, which is lower than pure NC, suggesting that part of these NC were dissolved in the tellurite glass. On the other hand, lifetimes from the G2 series exhibit higher values around 0.9 ms within the error analysis, which is an unexpected result since both glassy tellurite or crystalline lanthanum niobate environments should result in lower values. Since excitation and emission spectra already pointed out that NC are not completely dissolved in the tellurite matrix in these G2 samples but, on the other hand, Eu³⁺ are apparently feeling a more propitious neighborhood than in LaNbO₄ NC powders for higher lifetimes, one could understand the NC incorporation process by looking on the NC transformation over time in the tellurite glass: it is supposed that NC dissolve following a specific kinetic related with temperature, composition and viscosity. NC dissolution through diffusion of lanthanum, niobium and europium in the liquid tellurite glass is expected to be relatively slow because of the viscosity. Hence, low times could result to the formation of an amorphous lanthanum niobate domain between the tellurite environment and the inner still crystalline part of the NC.

Table 2. Refractive index of the glasses and Lifetime of samples: G1-775-5, G1-775-45, G2_{TT}-630-07 and G2_{TT}-700-07 ($\lambda_{exc} = 394$ nm and $\lambda_{em} = 612$ nm).

Sample	Refractive index n ($\lambda=543,3$ nm)	τ_{exp}	R ²
G1	2.0224	-	-
G2	2.0015	-	-
NC	2.2500	0.787 ± 0.007	0.998
G1-775-05	-	0.700 ± 0.043	0.928
G1-775-45	-	0.745 ± 0.042	0.939
G2 _{TT} -630-07	-	0.931 ± 0.045	0.96
G2 _{TT} -700-07	-	0.867 ± 0.044	0.954

Table 3. Radiative and non-radiative transitions probabilities and quantum efficiency.

Sample	A_{RAD} (ms^{-1})	A_{NRAD} (ms^{-1})	τ_{rad} (ms)	η
NC _{TT}	0.42	0.82	2.36	0.33
G1-775-05	0.41	0.83	2.43	0.29
G1-775-45	0.39	0.87	2.64	0.28
G2 _{TT} -630-07	0.48	0.62	2.09	0.44
G2 _{TT} -700-07	0.38	0.73	2.62	0.32

However, for longer times, the NC fully dissolve in the tellurite glass. In this sense, one could suggest that samples G2 belong to this intermediary NC state between fully crystalline particles and complete dissolution. In this case, such amorphous lanthanum niobate environment should give suitable conditions (refractive index and phonon energy) for longer Eu^{3+} lifetimes. One should also not neglect the fact that Eu^{3+} from the NC surface may have time for dissolution and experiment a tellurite environment of lower refractive index (Table 2). This lifetime increase could not be related with the higher alkali content in G2 samples since alkali incorporation in tellurite glasses promote the formation of TeO_3 units with an overall higher phonon energy of the glass matrix. In this sense, lower experimental lifetimes and quantum efficiencies should be expected³⁵.

Finally, probability values for radiative and non-radiative transitions, radiative lifetime and quantum efficiency were also estimated from the emission spectra (Table 3). Because of specific properties of electronic transitions from Eu^{3+} , emission bands can be used to access transition probabilities and resulting radiative (A_{RAD}) and non-radiative (A_{NRAD}) transition rates, as well as quantum efficiency (η). The radiative emission rate can be calculated by Equation 1, where A_{0-j} corresponds to the probability of each Eu^{3+} electronic transition and τ_{RAD} the radiative lifetime^{16,36}.

$$A_{\text{RAD}} = \sum A_{0-j} = \frac{1}{\tau_{\text{RAD}}} \quad (1)$$

A_{0-j} values can be found by Equation 2, in which $S_{0-\lambda}$ corresponds to the area under the ${}^5\text{D}_0 \rightarrow {}^7\text{F}_\lambda$ emission band obtained from the emission spectra (values for transitions $0 \rightarrow 5,6$ negligible), and σ_λ the energy of corresponding transition barycenter. In this case, transition $0 \rightarrow 1$ is used as a reference, since it occurs by MD and is virtually under no influence of the site in which the ion is inserted. For probability value A_{0-1} , a standard value of $A_{0-1} = 50 \text{ s}^{-1}$ was employed^{15,16,21,31}, considering a refractive index higher than 1.5 for the NC and the CG.

$$A_{0-j} = \frac{S_{0-\lambda}}{S_{0-1}} \frac{\sigma_1}{\sigma_\lambda} A_{0-1} \quad (2)$$

The non-radiative emission rate can then be obtained by Equation 3 and quantum efficiency by Equation 4, with τ_{exp} being the experimental lifetime.

$$A_{\text{NRAD}} = \frac{1}{\tau_{\text{exp}}} - A_{\text{RAD}} \quad (3)$$

$$\eta = \frac{A_{\text{RAD}}}{A_{\text{RAD}} + A_{\text{NRAD}}} = \frac{\tau_{\text{exp}}}{\tau_{\text{RAD}}} \quad (4)$$

Quantum efficiency values resumed in Table 3 are in good agreement with other spectroscopic data and display the same trend than experimental lifetimes. In fact, whereas G1 composite-glass present lower quantum efficiencies than the corresponding NC ($\eta = 0.33$), G1 samples exhibit higher values with G2_{TT}-630-07 reaching $\eta = 0.44$, suggesting again that low temperatures and times promote better Eu^{3+} environment in terms of luminescent properties when compared to both tellurite glasses and LaNbO_4 crystalline powders.

4. Conclusion

Composite-glasses were prepared by incorporating lanthanum niobate nanocrystals previously doped with Eu^{3+} ion ($\text{LaNbO}_4:\text{Eu}^{3+}$) in powdered tellurite glasses of two different molar compositions in the $\text{TeO}_2\text{-GeO}_2\text{-Nb}_2\text{O}_5\text{-K}_2\text{O-Li}_2\text{O}$ system. Several parameters such as nanocrystals/glass proportion, temperature and time, heat treatment of nanocrystals, were adjusted. All these parameters appeared to greatly influence CG transparency and amorphous/crystalline state. Glass transition temperature were helpful to confirm that longer temperatures and times progressively dissolve NC, as probed by the increase in Tg temperatures. Eu^{3+} spectroscopic investigations allowed to understand NC transformation in the tellurite glass as a function of time. In fact, both excitation and emission spectra point out that higher times and temperatures (G1 samples) promote an amorphous Eu^{3+} environment attributed to NC dissolution in the tellurite network whereas softer conditions (lower temperatures and times) give rise to an intermediary structural and chemical Eu^{3+} environment of higher symmetry. Under these conditions, experimental lifetimes and quantum efficiencies also depict an unexpected fact, showing improved Eu^{3+} luminescent properties in these materials when compared to starting NC powders (higher lifetime and quantum efficiency). Therefore, one could suggest that the outer part of NC is not dissolved in the tellurite network. As a consequence, a glassy lanthanum niobate phase with very propitious optical properties for Eu^{3+} luminescence is formed between the surrounding tellurite glass and inner crystalline domain of the NC. This investigative work paves the way for new materials methodologies and design not achievable by conventional heat-treatment of a precursor glass.

5. Acknowledgments

The authors would like to thank Brazilian funding agencies FAPEMIG, Brazil; FINEP, Brazil; CAPES, Brazil; FAPESP, Brazil; and CNPq, Brazil; for financial support.

6. References

- Llórdes A, Garcia G, Gazquez J, Milliron DJ. Tunable near-infrared and visible-light transmittance in nanocrystal-in-glass composites. *Nature*. 2013;500(7462):323-6. <http://dx.doi.org/10.1038/nature12398>.
- Zhao J, Zheng X, Schartner EP, Ionescu P, Zhang R, Nguyen T-L, et al. Upconversion nanocrystal-doped glass: a new paradigm for photonic materials. *Adv Opt Mater*. 2016;4(10):1507-17. <http://dx.doi.org/10.1002/adom.201600296>.
- Xu Y, Zhang X, Dai S, Fan B, Ma H, Adam J-L, et al. Efficient near-infrared down-conversion in Pr³⁺-Yb³⁺ codoped glasses and glass ceramics containing LaF₃ nanocrystals. *J Phys Chem C*. 2011;115(26):13056-62. <http://dx.doi.org/10.1021/jp201503v>.
- Blanc W, Choi YG, Zhang X, Nalin M, Richardson KA, Righini GC, et al. The past, present and future of photonic glasses: a review in homage to the United Nations International Year of glass 2022. *Prog Mater Sci*. 2023;134(1):101084. <http://dx.doi.org/10.1016/j.pmatsci.2023.101084>.
- Alzahrani AS. A review of glass and crystallizations of glass-ceramics. *Adv Mater Phys Chem*. 2022;12(11):261-88. <http://dx.doi.org/10.4236/ampe.2022.1211018>.
- Zhao J, Ebendorff-Heidepriem H. Direct doping of nanoparticles in glass shows potential for smart applications. Washington: SPIE; 2016. <http://dx.doi.org/10.1117/2.1201610.006708>.
- Li X, Guan Z, Duan Y, Shen R, Tian Y, Wang X, et al. Bright green up-conversion luminescence of LaNbO₄: Nd³⁺/Yb³⁺/Ho³⁺ phosphors under 808 nm and 980 nm excitations and the effects of dopant concentration. *J Lumin*. 2022;241(1):118524. <http://dx.doi.org/10.1016/j.jlumin.2021.118524>.
- Pugina RS, Hilário EG, Rocha EG, Silva-Neto ML, Das A, Caiuti JMA, et al. Nd³⁺:YAG microspheres powders prepared by spray pyrolysis: synthesis, characterization and random laser application. *Mater Chem Phys*. 2021;269(1):124764. <http://dx.doi.org/10.1016/j.matchemphys.2021.124764>.
- Xu Y, Xin Y, Shirai T. A novel one-step synthesis of bright luminescent silicon nanocrystals capped with hydrophobic surface. *Colloid Interface Sci Commun*. 2021;45(1):100547. <http://dx.doi.org/10.1016/j.colcom.2021.100547>.
- Wei S, Luo X, Wang L, Miao J. High-quality luminescent CsPbBr₃ perovskite nanocrystals prepared by a facile two-phase method. *Chem Phys Lett*. 2023;812(1):140262. <http://dx.doi.org/10.1016/j.cplett.2022.140262>.
- Nguyen H, Tuomisto M, Oksa J, Salminen T, Lastusaari M, Petit L. Upconversion in low rare-earth concentrated phosphate glasses using direct NaYF₄:Er³⁺, Yb³⁺ nanoparticles doping. *Scr Mater*. 2017;139(1):130-3. <http://dx.doi.org/10.1016/j.scriptamat.2017.06.050>.
- Lopez-Iscosa P, Ojha N, Aryal U, Pugliese D, Boetti NG, Milanese D, et al. Spectroscopic properties of Er³⁺-doped particles-containing phosphate glasses fabricated using the direct doping method. *Materials*. 2019;12(1):129. <http://dx.doi.org/10.3390/ma12010129>.
- Lahti V, Ojha N, Vuori S, Lastusaari M, Petit L. Preparation of glass-based composites with green upconversion and persistent luminescence using modified direct doping method. *Mater Chem Phys*. 2021;274(1):125164. <http://dx.doi.org/10.1016/j.matchemphys.2021.125164>.
- Ballato J, Ebendorff-Heidepriem H, Zhao J, Petit L, Troles J. Glass and process development for the next generation of optical fibers: a review. *Fibers*. 2017;5(1):11. <http://dx.doi.org/10.3390/fib5010011>.
- Freiria GS, Nassar EJ, Verelst M, Rocha LA. Influence of the electrostatic filter field on particle size control of (La_{0.98}Eu_{0.01}Bi_{0.01})NbO₄ red phosphor prepared using spray pyrolysis. *J Lumin*. 2016;169:844-9. <http://dx.doi.org/10.1016/j.jlumin.2015.06.022>.
- Freiria GS. Obtenção de Niobato de lantânio contendo íons Eu³⁺ e Dy³⁺ pelo processo de pirólise de aerossol [dissertation]. Franca: Universidade de Franca; 2017 [cited 2023 Aug 22]. Available from: <https://repositorio.up.edu.br/jspui/handle/123456789/451>
- Cui Z, Deng G, Xu P, Liu X, Yang M, Wang O. Preparation and luminescence properties investigation of Eu³⁺, Tb³⁺-doped LaNbO₄:RE³⁺ (RE=Eu, Eu/Tb, Tb). *J Mater Sci Mater Electron*. 2022;33(1):11174-83. <http://dx.doi.org/10.1007/s10854-022-08093-0>.
- Dwivedi A, Roy A, Rai SB. Photoluminescence behavior of rare earth doped self-activated phosphors (i.e. niobate and vanadate) and their applications. *RSC Advances*. 2023;13(24):16260-71. <http://dx.doi.org/10.1039/D3RA00629H>.
- Anan'eva GV, Bakhshieva GF, Karapetyan VE, Morozov AM, Sychev EM. Crystal growth and optical characteristics of lanthanian fergusonite. In: Sheftal' NN, Givargizov EI, editors. Growth of crystals. Boston: Springer; 1975. http://dx.doi.org/10.1007/978-1-4684-1689-3_35.
- Singh SP, Sontakke AD. Transparent glass-ceramics. *Crystals*. 2021;11(2):156. <http://dx.doi.org/10.3390/cryst11020156>.
- Barbosa JS, Batista G, Danto S, Fargin E, Cardinal T, Poirier G, et al. Transparent glasses and glass-ceramics in the ternary system TeO₂-Nb₂O₅-PbF₂. *Materials*. 2021;14(2):317. <http://dx.doi.org/10.3390/ma14020317>.
- Dai S, Wu J, Zhang J, Wang G, Jiang Z. The spectroscopic properties of Er³⁺-doped TeO₂-Nb₂O₅ glasses with high mechanical strength performance. *Spectrochim Acta A Mol Biomol Spectrosc*. 2004;62(1-3):431-7. <http://dx.doi.org/10.1016/j.saa.2005.01.011>.
- Hammami I, Gavinho SR, Pádua AS, Lança MC, Borges JP, Silva JC, et al. Extensive investigation on the effect of niobium insertion on the physical and biological properties of 45S5 bioactive glass for dental implant. *Int J Mol Sci*. 2023;24(6):5244. <http://dx.doi.org/10.3390/ijms24065244>.
- Siripuram R, Rao PSG, Sripada S. Influence of nano crystalline behavior of Nb₂O₅ - Sb₂O₃ - TeO₂ glass ceramics on structural and thermal studies. *Mater Today Proc*. 2021;46(14):6344-57. <http://dx.doi.org/10.1016/j.matpr.2020.05.818>.
- Thomas RL, Nampoory VPN, Radhakrishnan P, Thomas S. Laser induced fluorescence in europium doped zinc tellurite glasses. *Optik*. 2013;124(22):5840-2. <http://dx.doi.org/10.1016/j.ijleo.2013.04.008>.
- Jian L, James RD. Prediction of microstructure in monoclinic LaNbO₄ by energy minimization. *Acta Mater*. 1997;45(10):4271-81. [http://dx.doi.org/10.1016/S1359-6454\(97\)00080-3](http://dx.doi.org/10.1016/S1359-6454(97)00080-3).
- Hsiao YJ, Fang TH, Chang YS, Chang YH, Liu CH, Ji LW, et al. Structure and luminescent properties of LaNbO₄ synthesized by sol-gel process. *J Lumin*. 2006;126(2):866-70. <http://dx.doi.org/10.1016/j.jlumin.2007.01.005>.
- Hadidi K, Hancke R, Norby T, Gunnæs AE, Løvvik OM. Atomistic study of LaNbO₄; surface properties and hydrogen adsorption. *Int J Hydrogen Energy*. 2011;37(8):6674-85. <http://dx.doi.org/10.1016/j.ijhydene.2012.01.065>.
- Hrabovsky J, Desevedavy F, Strizik L, Gadret G, Kalenda P, Frumarova B, et al. Glass formation and properties of the TeO₂-ZnO-BaO tellurite optical glasses. *J Non-Cryst Solids*. 2022;582(1):121445. <http://dx.doi.org/10.1016/j.jnoncrsol.2022.121445>.
- Tran TNL, Chiasera A, Lukowiak A, Ferrari M. Eu³⁺ as a powerful structural and spectroscopic tool for glass photonics. *Materials*. 2022;15(5):1847. <http://dx.doi.org/10.3390/ma15051847>.
- Binnemans K. Interpretation of europium (III) spectra. *Coord Chem Rev*. 2014;295:1-45. <http://dx.doi.org/10.1016/j.ccr.2015.02.015>.

32. Rakov N, Amaral DF, Guimarães RB, Maciel GS. Spectroscopic analysis of Eu^{3+} - and $\text{Eu}^{3+}:\text{Yb}^{3+}$ -doped yttrium silicate crystalline powders prepared by combustion synthesis. *J Appl Phys.* 2010;108(7):073501. <http://dx.doi.org/10.1063/1.3489992>.
33. Calefi PC, Silva RRC, Reis MJ, Nassar EJ. A luminescência do eu^{3+} para elucidação estrutural: apropriação e utilização de conceitos e linguagens por estudantes de iniciação científica. *Iluminart.* 2014 [cited 2023 Aug 22];6(12):9-24. Available from: <http://revistailuminart.ti.srt.ifsp.edu.br/revistailuminart/index.php/iluminart/article/view/207>
34. Matias CR, Nassar EJ, Verelst M, Rocha LA. Synthesis and CHARACTERIZATION of $\text{Nb}_2\text{O}_5:\text{La}^{3+},\text{Eu}^{3+}$ phosphors obtained by the non-hydrolytic sol-gel process. *J Braz Chem Soc.* 2015;26:2558-70. <http://dx.doi.org/10.5935/0103-5053.20150242>.
35. Rimbach AC, Steudel F, Ahrens B, Schweizer S. Tb^{3+} , Eu^{3+} , and Dy^{3+} doped lithium borate and lithium aluminoborate glass: glass properties and photoluminescence quantum efficiency. *J Non-Cryst Solids.* 2018;499:380-6. <http://dx.doi.org/10.1016/j.jnoncrysol.2018.07.029>.
36. Marcondes LM, Santagneli SH, Manzani D, Cassanjes FC, Batista G, Mendoza VG, et al. High tantalum oxide content in Eu^{3+} -doped phosphate glass and glass-ceramics for photonic applications. *J Alloys Compd.* 2020;842(1):155853. <http://dx.doi.org/10.1016/j.jallcom.2020.155853>.